in vivo [^{123}I]β-CIT binding to dopamine transporters in healthy human subjects. *J Cereb Blood Flow Metab* 1994;14:982–994.

44. Salmon E, Brooks DJ, Leenders KL, et al. A two-compartment description and kinetic procedure for measuring regional cerebral [^{11}C]nomifensine uptake using positron emission tomography. *J Cereb Blood Flow Metab* 1990;10:307–316.

45. Brücke T, Asenbaum S, Pozzera A, et al. Dopaminergic nerve cell loss in Parkinson's disease quantified with [I-123]-β-CIT and SPECT correlates with clinical findings. *Mov Disord* 1994;9(suppl 1):120.

46. Garnett ES, Nahmias C, Firnau G. Central dopaminergic pathways in hemiparkinsonism examined by positron emission tomography. *Can J Neurol Sci* 1984;11:174–179.

47. Karbe H, Holthoff V, Huber M, et al. Positron emission tomography in degenerative disorders of the dopaminergic system. *J Neural Transm* 1992;4:121–130.

48. Marek KL, Seibyl JP, Zoghbi S, et al. Iodine-123-β-CIT/SPECT imaging demonstrates bilateral loss of dopamine transporters in hemi-Parkinson's disease. *Neurology* 1996;46:231–237.

49. Kempster PA, Gibb WRG, Stern GM, Lees AJ. Asymmetry of substantia nigra neuronal loss in Parkinson's disease and its relevance to the mechanism of levodopa related motor fluctuations. *J Neurol Neurosurg Psychiatry* 1989;52:72–76.

50. Heinonen EH, Anttila MI, Lammintausta RAS. Pharmacokinetics and clinical pharmacology of selegilin. In: Szelenyi, ed. *Inhibitors of monoamine oxidase B. Pharmacology and clinical use in neurodegenerative disorders.* Basel: Birkhäuser; 1993:201–213.

51. Xu C, Coffey LL, Reith ME. Translocation of dopamine and binding of 2-beta-carbomethoxy-3-beta-(4-fluorophenyl) tropane (WIN 35,428) measured under identical conditions in rat striatal synaptosomal preparations. Inhibition by various blockers. *J Biochem Pharmacol* 1995;49:339–350.

Regional Stability of Cerebral Blood Flow Measured by Repeated Technetium-99m-HMPAO SPECT: Implications for the Study of State-Dependent Change

Georg Deutsch, James M. Mountz, Charles R. Katholi, Hong-Gang Liu and Lindy E. Harrell

Division of Nuclear Medicine, Department of Radiology; Department of Biostatistics and Mathematics; and Department of Neurology, University of Alabama at Birmingham Medical Center, Birmingham, Alabama

The replicability of resting state rCBF has implications for the analysis of cerebral activation protocols and the interpretation of rCBF in disease states. This study examined the stability of rCBF as measured by two resting state ^{99m}Tc-HMPAO brain SPECT scans with an emphasis on examining the contribution of specific cerebral regions to within and between subjects variance. **Methods:** Nine normal, medically healthy subjects underwent two ^{99m}Tc-HMPAO brain SPECT scans under identical conditions separated by 48 hr. A reference system and semiautomated computer ROI method was used to enable accurate alignment and cortical analysis of the two scans. **Results:** Mean within-subject difference between Scans 1 and 2 was 2.8% (range 0%-7.8%) for the 36 cortical ROIs. The mean between-subject coefficient of variation was 10% (range 7%-15%) for these ROIs. Correlation analysis of rCBF pattern replication for all slice levels yielded a highly significant overall consistency of pattern within subjects (Pearson r = 0.698, p = 0.0001). Variance component analysis revealed regional heterogeneity in between-subjects variance, with significantly greater variability found in frontal regions. The within-subject repeated measures variability was not significantly different across regions. **Conclusion:** Good within-subject 48-hr replicability indicates that individual resting state rCBF reflects fairly stable, subject-specific factors. This also justifies comparing state-dependent studies separated by a modest length of time. Although individual patterns of rCBF replicate well, the larger contribution of frontal regions to normal between-subjects variance makes evaluating the frontal effects of disease or activation more difficult.

Key Words: normal cerebral blood flow; activation states; technetium-99m-HMPAO; SPECT; rCBF

J Nucl Med 1997; 38:6–13

Activation studies of regional cerebral blood flow (rCBF) during stimulation, motor activity, psychological tasks and other state manipulations have become a prominent part of functional neuroimaging research. Such investigations were originally conducted using ^{133}Xe cortical blood flow measures and later using ^{15}O-water rCBF PET, since these methods allow relatively rapid sequential repeat measures on the same subject. The ability to study the rCBF effects of several different conditions in the same session is clearly convenient and possibly reduces the errors associated with repositioning subjects in protocols involving testing sessions separated in time. Sequential studies are also thought to be best suited for activation research because it is generally believed that proximity in time reduces variability associated with uncontrolledfor changes in a subject's physiology, mental state and mood, i.e., state dependent factors not being specifically evaluated by the experimental protocol.

SPECT tracers such as ^{99m}Tc-HMPAO are not readily suited for immediately repeated studies because clearance of the tracer from cerebral tissue is essentially dependent on radioactive decay (based on a 6-hr physical half-life in the case of ^{99m}Tc). The lack of redistribution and clearance is at the same time an extremely useful property, allowing investigators to capture a state present at the time of ^{99m}Tc-HMPAO injection and scan the subject later. This offers advantages for experimental situations in which the state to be studied is difficult to capture, achieve or control within a scanner, such as an ictal seizure state (*1*), psychiatric research paradigms involving complex state changes (*2*) and for situations where anesthesia may be required to properly scan an uncooperative patient but where the anesthetic may mask the effects of the disease state under study, such as in the case of autistic patients (*3*). Brain SPECT scans using ^{99m}Tc-HMPAO can be used for activation protocols either by a split dose technique, in which one condition is evaluated using a low ^{99m}Tc-HMPAO dose, and another condition is scanned using a much higher dose, or by separating each study condition by two days, allowing the initially injected tracer to decay. The former method unfortunately results in the

low dose condition being of poorer image quality, whereas the latter method potentially introduces a greater number of uncontrolled-for changes accompanying the required separation in time; although it can also be argued that separation in time reduces fatigue and potential habituation effects (4).

Analyzing stress or activation effects in groups of subjects typically involves a repeated measures design that, in effect, uses each subject as their own control and evaluates state-induced changes relative to each subject's baseline rCBF pattern. Although more recently there has been a shift in emphasis to analyzing the covariance structure of activation datasets as opposed to just identifying maximal changes, most investigators continue to depend on either baseline or control state studies in analyzing activation protocols (5–7). Analysis protocols such as IAPS (intersubject averaging of paired-image subtractions) (8) and the ANCOVA-based statistical parametric mapping (SPM) (9) that are thought to accurately represent the intrasubject activation signal after removal of intersubject effects and any remaining (presumed random) signal variation, nevertheless, depend on baseline control conditions for each subject. Principal component analysis (PCA) methods also typically incorporate resting state baselines in the analysis of activation datasets (10–11).

Adjusting for individual resting state rCBF differences assumes that resting state levels reflect stable, subject specific, physiological differences more than idiosyncratic factors that vary from session to session. In addition, stability of the normal rCBF pattern is critical in establishing quantitative criteria for rCBF markers of disease.

Earlier studies of cortical blood flow using ^{133}Xe inhalation documented a general consistency in the distribution of resting state rCBF across subjects, with most investigators reporting a hyperfrontal gradient in flow (12–16). Some regional differences in the variability of rCBF associated with repeat measures was also reported, with dedicated sensory motor cortex showing the most stability (13). Very little has been published regarding the *pattern* replicability of resting state rCBF measurements using PET or SPECT. Several PET studies reported on within-subject replicability of mean (whole brain or global) absolute blood flow, with whole brain differences claimed to be < 5% (17) or to be nonsignificant (18,19). A more recent ^{15}O-H$_2$O PET study specifically looking at resting state rCBF reproducibility also reported good within-subject replication of mean absolute flow in two successive scans, with absolute percent difference averaging 7.2% (20). In reporting on regional flow pattern consistency, the study concluded that within-subject reproducibility was good because none of 14 selected ROIs had a statistically significant different rCBF between the two measurements. A SPECT study evaluating ^{99m}Tc-bicisate (ECD) reported on 48-hr replicability of this tracer in a similar manner, claiming a lack of significant differences in 14 regions in a repeated measures design protocol (21).

In the present study, we evaluated resting state rCBF pattern replicability as measured by ^{99m}Tc-HMPAO brain SPECT scans separated by two days. The degree of replicability would determine the extent to which such rCBF SPECT scans (and other imaging methods as well) could be used to directly compare the rCBF effects of different states studied on different days. The study was to determine whether specific cerebral regions contributed a disproportionate share to overall subject-to-subject variance as well as to variability in repeated measures of the same subject. Any such consistencies found would have implications for the analysis of activation protocols and certain disease states.

SUBJECTS AND METHODS

Subjects were recruited from the normal control subject pool of the UAB Alzheimer's Disease Center where they had been evaluated for several NIH-funded research protocols concerning aging and dementia. Each subject had undergone comprehensive neurological and neuropsychological evaluation, as well as routine medical exams and anatomic scans of the brain, which were in each case normal. There were five women and four men, with an age range of 55–71 and mean age of 59.7 ± 5.8 yr. All volunteers fully consented to these procedures, which satisfied institutional review board criteria.

On the day of each scan, subjects were briefed and prepared in a quiet testing room where a small heparin lock needle was inserted into a prominent antecubital fossa vein. The subject was then asked to relax for 15 min in a supine resting state on a comfortable bed. An approximation of arterial carbon dioxide levels was obtained by end tidal CO_2 sampling via mask for a period of one minute such that changes in respiration and blood CO_2 levels between the two scans would be documented. After another 5 min of rest, the subject received 30 mCi ^{99m}Tc-HMPAO intravenously. The subject remained in the quiet resting state for another 5 min while the tracer was incorporated into the brain (the irreversible retention of tracer in brain tissue reflects the regional cerebral perfusion at a time approximately between 5 to 60 sec postintravenous bolus injection) (22). Each subject was then asked to rate themself regarding predominant thoughts, mood, anxiety and sleepiness during the time of tracer injection. This information was used to document any unusual changes in mood or mental state between Scans 1 and 2.

Subjects were then taken to the SPECT scanner. A reference system device to permit coalignment of images from the two scanning sessions was precisely positioned on the subject's head. This standardized and validated device (23–25) uses two triangles attached to a glasses-like framework, the base of which is positioned between the auditory meatus and lateral canthus of the eye. Thin intravenous tubing, which courses along each triangle edge, is injected with 1.25 μCi/cm ^{99m}Tc-NaTcO$_4$ (or another appropriate contrast agent in the case of CT or MRI scans) and forms sequential external points on transverse scan sections allowing for accurate coalignment and any necessary reorientation between imaging sessions. Scanning was performed on the ADAC dual-headed Genesis Anger gamma camera (ADAC Laboratories, Milpitas, CA) by sampling a 25-cm field of view over 360°. Each detector was equipped with a low-energy, high-resolution collimator. Angular projection sampling was performed using 128 total projections (64 stops/head on the dual-head camera or approximately 3° sequential angular projection per stop). Data are projected into a 128 × 128 pixel matrix size that results in pixel dimension of 1.96 mm on edge.

Scan reconstruction was performed on the ADAC Pegasus work station using a Butterworth filter with a frequency cutoff of 0.225 cycles per centimeter, order 6 (26). Images were attenuation corrected using the Chang algorithm. Images were obliquely reconstructed parallel to and sequentially above the canthomeatal line. Every other plane slice was added in the oblique transverse (as well as coronal and sagittal) sections to obtain a final image plane thickness of 3.92 mm for ROI analysis. The in-plane resolution for ROI analysis retained the pixel dimension size of 1.96 mm on edge for better ROI border delineation. Using the acquisition parameters described above, the average in-plane axial resolution is approximately 8.5 mm full width half-maximum.

After image reconstruction, a semiautomated routine was applied to the midcerebellar slice and to slices 3.5, 5.5 and 7.5 cm above and parallel to the canthomeatal line as determined from the reference system. The semiautomated routine draws an outer

boundary of the cortex at a 50% count threshold of the maximum counts per pixel of the slice under analysis and an inner boundary 8 pixels deep (1.57 cm). The resulting annulus is then subdivided by the algorithm into 12 equal angular sectors, and the operator chooses among several methods available for calculating count density in each ROI for display and storage of data (27–30). For the data presented here, the average of the top 10% maximum count pixels was calculated for each ROI and normalized to the maximum counts per pixel in the midcerebellar slice to minimize the possibility of obtaining count data from statistically outlying pixels. Figure 1A shows the location of the transverse slices and subdivided sectors on a diagram of the brain. Figure 1B shows an example of the computer automated routine applied to level CM + 5.5 of the SPECT image of one subject.

For subcortical regions, the slice through the center of each structure was chosen by reference to an MRI or CT scan. The boundaries of the caudate nuclei and thalami were demarcated by coregistration of the edge of the structures from the CT or MRI scan (23–25). The average of the top 10% maximum count pixels was then calculated for each subcortical ROI and normalized to the maximum counts per pixel in the midcerebellar slice.

On the second scan session, which followed exactly 48 hr after the first scan session in all nine subjects, identical patient preparation, injection and scanning procedures were performed, and each subject was again debriefed regarding predominant thoughts, mood and anxiety level during the time of tracer injection.

Data Analysis

Analysis involved estimation of between- and within-subject variance components and comparison of within-subject rCBF pattern replication (concordance) at each of three slice levels using correlation techniques. Both the Pearson correlation method and Kendall's Tau were used. The latter provides a more appropriate measure of the concordance of rCBF patterns. Variance estimates were compared region by region to determine where there were significant differences in between- and within-subject components. Within subject variance across regions was compared using the maximum F statistic.

Replicability of regional rCBF values in each ROI was assessed using pairwise t-tests. P value for significance was set to 0.001 using Bonferroni correction for multiple comparisons (in this case 40). Fisher's procedure for calculating pooled p values for paired t-tests was then used to compare the replicability of each entire slice level. Simple correlations for each individual ROI were also calculated to allow comparison with other published reports using such analyses.

RESULTS

Table 1 presents the mean normal brain SPECT rCBF data for 36 cortical regions and four subcortical regions from Session 1 and also shows the average difference between Sessions 1 and 2 for each region within a subject. It can serve as normal control data for other investigators using the UAB or a similar ROI method. The mean within-subject difference between Scans 1 and 2 was 2.8% for the 36 cortical ROIs. The mean between-subject coefficient of variation (mean divided by s.d.) was 10% for these ROIs.

None of the subjects felt that there was any substantive difference in their mental state between the two sessions and this was reflected in equivalent scores on the simple rating scales used to quantitate self appraised mood, anxiety and sleepiness. Group mean end tidal CO_2 was virtually identical for session 1 (38.1 ± 2.3 mmHg) and session 2 (37.9 ± 2.5 mmHg), indicating no tendency to alter respiratory patterns and blood gas influences on global CBF.
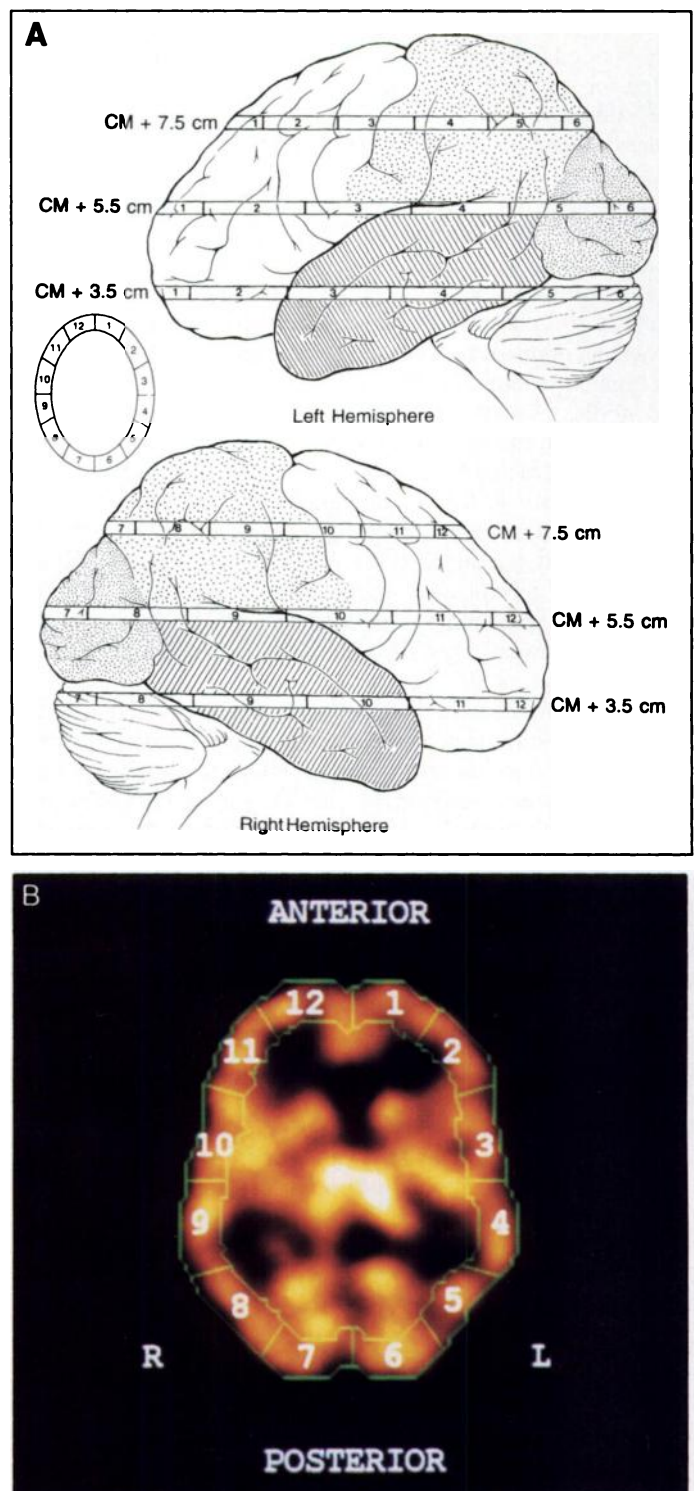

FIGURE 1. (A) Diagrams showing lateral views of the left and right hemispheres and indicating the anatomical locations of the three horizontal brain sections used for ROI analysis. The sections are at 3.5, 5.5 and 7.5 cm above the canthomeatal (CM) line. (B) A ^{99m}Tc-HMPAO brain SPECT scan section of a normal subject illustrating the method for obtaining circumferential cortical ROIs. The outer brain edge boundary is demarcated at the 50% count per pixel threshold and subdivided into ROIs by a computer-automated procedure described in the text.

Figure 2 shows the repeat scan images for one subject. The two sets of images were reconstructed to be accurately co-aligned, based on external fiduciary marks generated by the reference system.

TABLE 1
Normal Brain SPECT rCBF Data for 36 Cortical and 4 Subcortical Regions

	Region at level CM + 3.5				Region at level CM + 5.5				Region at level CM + 7.5			
	Scan 1		Scan 1:Scan 2 % Difference*		Scan 1		Scan 1:Scan 2 % Difference*		Scan 1		Scan 1:Scan 2 % Difference*	
Region	Mean	s.d.	Mean	s.d.	Mean	s.d.	Mean	s.d.	Mean	s.d.	Mean	s.d.
1	0.810	0.084	4.9	7.4	0.861	0.068	1.2	3.5	0.899	0.061	1.1	6.7
2	0.881	0.112	4.5	10.2	0.882	0.076	2.3	3.4	0.896	0.080	1.1	10.0
3	0.831	0.096	1.2	10.8	0.878	0.057	3.4	6.8	0.842	0.039	1.2	7.1
4	0.794	0.084	1.3	7.6	0.852	0.029	1.2	7.0	0.829	0.045	1.2	6.8
5	0.857	0.036	3.5	7.0	0.807	0.063	1.2	7.4	0.850	0.053	5.9	7.0
6	0.958	0.052	2.1	9.4	0.869	0.076	2.3	6.9	0.848	0.103	4.7	7.1
7	0.941	0.058	0.0	6.4	0.875	0.054	0.0	3.4	0.911	0.091	7.7	6.6
8	0.899	0.067	4.5	6.7	0.843	0.072	5.9	7.1	0.865	0.076	5.8	6.9
9	0.832	0.081	1.2	7.2	0.869	0.079	3.5	3.5	0.869	0.064	5.7	6.9
10	0.895	0.071	1.1	10.1	0.903	0.088	2.2	3.3	0.851	0.053	1.2	7.0
11	0.900	0.107	7.8	6.7	0.882	0.091	3.4	3.4	0.902	0.073	0.0	6.6
12	0.867	0.093	3.5	3.5	0.885	0.084	2.3	6.8	0.926	0.073	3.2	3.2
Lt. caudate	0.965	0.032	9.3	10.2								
Rt. caudate	0.923	0.068	8.7	8.8								
Lt. thalamus	0.954	0.063	9.8	10.3								
Rt. thalamus	0.969	0.064	9.5	10.3								

*Within subject, [(Scan 2)-(Scan 1)]/Scan 1.
CM + 3.5, 5.5, 7.5 = canthomeatal line plus 3.5, 5.5 and 7.5 cm.

Individual ROI replicability

Within-subject changes in rCBF between Scans 1 and 2 were not significant for any of the 40 regions analyzed. Table 2 shows the results of paired t-test analysis and correlation analysis comparing Scan 1 to Scan 2 values for each ROI. (Cortical ROI 9 at level CM + 5.5 showed the highest probability of a true scan-to-scan difference, p = 0.03, but this fell substantially short of the p = 0.001 value required when correcting a p = 0.05 significance level for 40 comparisons and is thus most likely spurious.) This analysis is similar to the data presented by Mathew et al. (20) for two consecutive ^{15}O-H$_2$O PET scans and compares favorably, i.e., both the study using consecutive scans and our study using scans separated by 2 days showed a lack of significant differences in regions analyzed. Our analysis, however, went beyond this and evaluated the concordance of the patterns of flow at three levels, as well as searched-for differences in variance across regions.

Pattern Replicability

Correlation analysis of rCBF *pattern* replication for all slice levels yielded a highly significant overall consistency of pattern within subjects (Pearson r = 0.698, p = 0.0001). Replication was best for level CM + 7.5 (only two subjects showed less than significant pattern correlation) and worst for level CM + 5.5 (four subjects showed less than significant correlation). Table 3 shows both Pearson and Kendall's correlation for each subject for each slice level. To further compare the reproducibility of each of the three brain levels, pooled p values were calculated from the paired t-tests for each cortical ROI comprising each respective slice level. Level CM + 7.5 showed the best reproducibility (worst pooled probability for significant difference: χ^2 (24) = 18.0015; p = 0.8029). Level CM + 5.5 showed the poorest reproducibility (best pooled probability for a significant difference: χ^2 (24) = 33.8987; p = 0.0866). Level CM + 3.5 showed a p = 0.3965 probability (χ^2 (24) = 25.1735) for a significant difference in repeated measures.

Figure 3 illustrates the circumferential cortical rCBF profile at level CM + 3.5 for three subjects. Despite the substantial
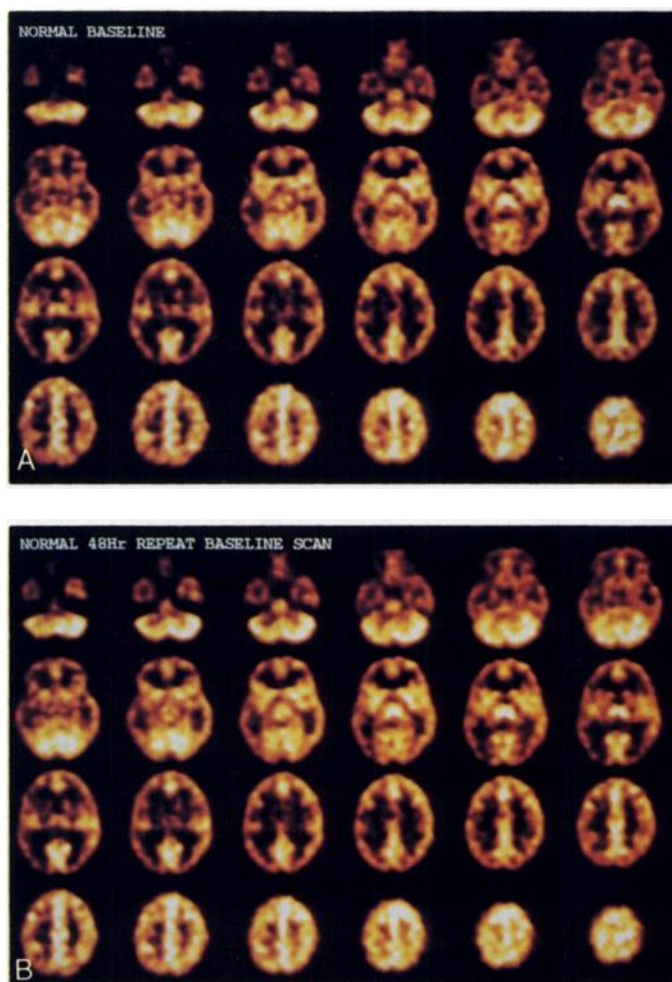

FIGURE 2. (A) Sequential ^{99m}Tc-HMPAO brain SPECT scans in transverse sections for a normal subject. (B) Technetium-99m-HMPAO brain SPECT of the subject shown in (A) conducted 48 hr after the first scan. Qualitative inspection shows distribution of tracer uptake in cortical giri and subcortical gray matter to be similar in the two scans.

TABLE 2
Regional rCBF Reproducibility: Individual ROI Values from Scans 1 and 2 Compared Through t-test and Correlation Analysis

Region	CM + 3.5		CM + 5.5		CM + 7.5	
	t-test	corr.	t-test	corr.	t-test	corr.
1	0.390	0.920	0.777	0.894	0.656	0.779
2	0.525	0.887	0.537	0.884	0.857	0.884
3	0.259	0.540	0.543	0.563	0.700	0.574
4	0.366	0.792	0.706	0.428	0.298	0.530
5	0.500	0.470	0.156	0.758	0.835	0.349
6	0.518	0.446	0.572	0.505	0.091	0.767
7	0.424	0.773	0.288	0.655	0.505	0.522
8	0.394	0.677	0.090	0.256	0.827	0.616
9	0.623	0.630	0.030	0.745	0.457	0.757
10	0.144	0.694	0.120	0.557	0.760	0.733
11	0.268	0.247	0.112	0.813	0.401	0.739
12	0.170	0.880	0.296	0.857	0.237	0.849
	t-test	corr.				
Rt. caudate	0.229	0.540				
Lt. caudate	0.484	0.750				
Rt. thalamus	0.764	0.730				
Lt. thalamus	0.360	0.650				

Note that correlations generally appear best for frontal regions (i.e., regions 1, 2, 11, 12) but are not necessarily consistent with the worst t-test probabilities for a significant difference.

between-subject variability, the repeat scan profiles replicate each subject's initial pattern quite well.

Variance Component Analysis

An analysis of variance components revealed greater between-subject variability than within. Figure 4 graphs the within- and between-subject variability for each of the three slice levels. The within-subject repeated measures variability was not significantly different across regions (maximum F-statistic). Between-subjects regional variance was much more heterogeneous, with significantly greater variability found in three frontal regions in each of the slice levels. Figure 4 shows the probability value for the difference in between- and within-subjects variance for the regions concerned.

Table 4 shows the variance components for the subcortical nuclei (left and right caudate and thalamus). Between- and within-subjects variability was not significantly different for these structures although the trend was for between-subject variability to actually be smaller. This reflects a tendency for run-to-run variance to overshadow the relatively high stability of these structures across subjects. The pooled p value for paired t-tests of these four nuclei was p = 0.5388 χ^2 (8) = 6.9799), indicating a moderately good reproducibility on successive scans.

Gender Effects

In estimating variance components, we assumed that the data of men and women was poolable. This assumption seemed reasonable due to the fact the data was normalized (to each subject's cerebellar flow) and thus not dependent on absolute flow differences, for which there is evidence of sex differences (6,16,31). Although we did not have a large enough sample to justify a full variance component analysis by sex, we explored the data to see if both men and women had similar variance findings as the grouped data in order to rule out a possible sex difference explanation for the greater between-subject frontal variance. The same pattern of results, i.e., variance component differences in the same direction, was seen in each group. Figures 5A and 5B illustrate the SPECT images of two subjects with very different patterns of frontal rCBF, both of whom are

women. These figures also show the consistency in this difference across multiple transverse slices.

DISCUSSION

The relative homogeneity of variance across regions within subjects provides justification for the use of parametric multivariate methods in repeated measures ^{99m}Tc-HMPAO brain SPECT protocols, including evaluation of activation or state dependent changes. The reproducibility or consistency of the resting rCBF pattern within a subject at two different testing sessions also justifies the use of activation paradigms where there may be a separation in time between scans. The within-subject reproducibility in our temporally separated resting state rCBF measurements is comparable to that observed in two successive resting state PET rCBF studies (20) and leads us to question the assumption that proximity in time is vital to reducing nonspecific variability or noise. In fact, it is just as likely that factors such as habituation (4), fatigue and impatience play a more prominent role in contributing uncontrolled-for variability in protocols involving successive studies than in protocols in which studies are separated in time.

Several previous studies have reported replicability data for rCBF for several ROI configurations, concluding that replicability was good since no region had a statistically significant different rCBF between the two measurements (20,21). The absence of significant regional differences between scan sessions attests to a reasonable degree of consistency but does not rigorously address the reproducibility issue nor in any way identify the nature of subject-to-subject rCBF variability.

It is of interest that Matthew et al. (20) reported best (within-subject) correlations for the frontal regions, while we found these regions to have the greatest across-subject variability. While these findings are not at odds, we were curious as to whether there was some reason for this apparent inverse relationship. Our correlation data (Table 2) showed the same findings, i.e., within-subject regional correlations on repeated measures were greatest for the frontal regions, but further inspection indicated that this was, in fact, an artifact of the greater range in flow values in frontal regions across subjects,

TABLE 3
rCBF Pattern Reproducibility: Pearson and Kendall's Correlations for Each Subject's Circumferential rCBF Profile at Each Slice Level, Comparing Scans 1 and 2

Subject	Level (CM+)	Pearson Corr. (p=)	Kendall Corr. (p=)
BR	3.5	0.42 (0.170)	0.25 (0.270)
	5.5	0.61 (0.030)	0.37 (0.098)
	7.5	0.83 (0.000)	0.74 (0.000)
	All	0.687 (0.0001)	0.477 (0.0001)
CE	3.5	0.82 (0.009)	0.51 (0.022)
	5.5	0.32 (0.310)	0.25 (0.260)
	7.5	0.42 (0.170)	0.19 (0.400)
	All	0.570 (0.0003)	0.365 (0.0023)
CJ	3.5	0.44 (0.150)	0.33 (0.140)
	5.5	0.25 (0.420)	0.18 (0.410)
	7.5	0.91 (0.000)	0.75 (0.000)
	All	0.572 (0.0003)	0.414 (0.0005)
GM	3.5	0.44 (0.150)	0.34 (0.090)
	5.5	0.92 (0.000)	0.69 (0.002)
	7.5	0.61 (0.030)	0.38 (0.090)
	All	0.709 (0.0001)	0.460 (0.0001)
KP	3.5	0.83 (0.000)	0.79 (0.000)
	5.5	0.40 (0.200)	0.26 (0.240)
	7.5	0.51 (0.088)	0.29 (0.209)
	All	0.492 (0.0020)	0.346 (0.0036)
LD	3.5	0.90 (0.000)	0.62 (0.006)
	5.5	0.86 (0.000)	0.82 (0.000)
	7.5	0.85 (0.000)	0.74 (0.003)
	All	0.876 (0.0001)	0.742 (0.0001)
LO	3.5	0.91 (0.000)	0.75 (0.001)
	5.5	0.16 (0.620)	0.01 (0.940)
	7.5	0.11 (0.700)	0.00 (1.00)
	All	0.376 (0.0240)	0.255 (0.0309)
MM	3.5	0.83 (0.000)	0.71 (0.000)
	5.5	0.95 (0.000)	0.66 (0.003)
	7.5	0.79 (0.002)	0.54 (0.016)
	All	0.837 (0.0001)	0.607 (0.0001)
WJ	3.5	0.92 (0.000)	0.72 (0.001)
	5.5	0.62 (0.031)	0.36 (0.110)
	7.5	0.68 (0.014)	0.61 (0.006)
	All	0.841 (0.0001)	0.641 (0.0001)
	Grand	0.700 (0.0001)	0.497 (0.0001)

All = correlation for pattern consisting of all three slices within a subject, i.e., a 36 ROI ribbon.

Grand = correlation for pattern consisting of all 27 slices from all subjects, i.e., a 324 ROI ribbon.
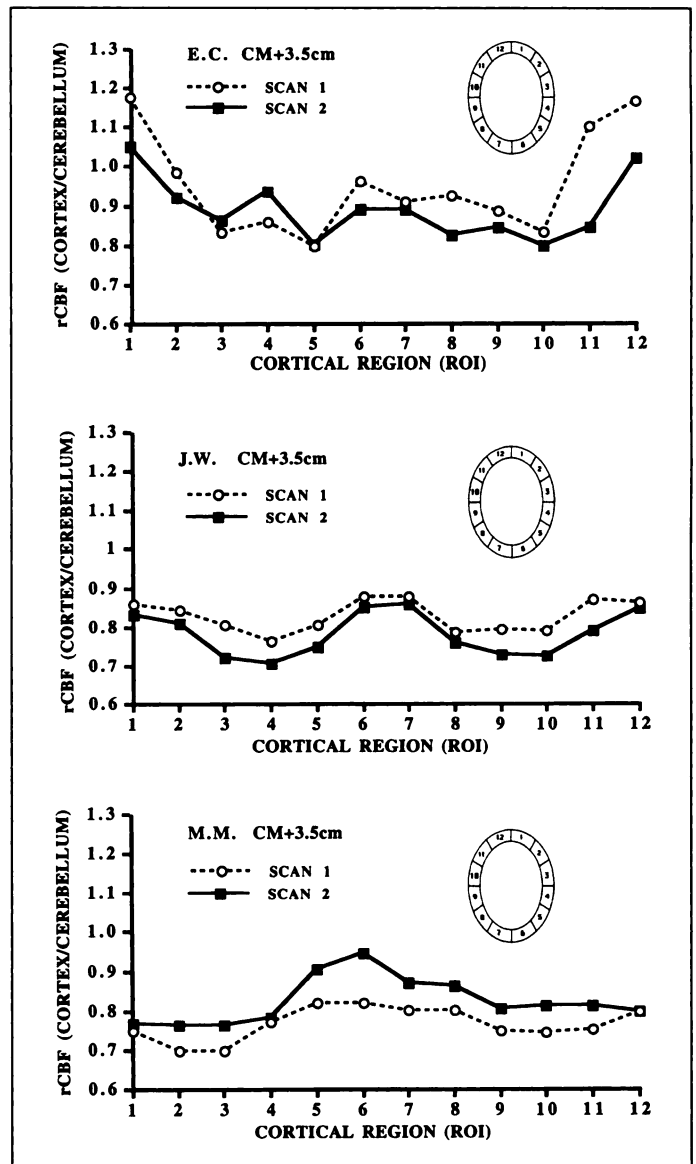

FIGURE 3. Cortical circumferential profiles at level CM + 3.5 for three subjects, comparing Scan 1 with Scan 2. Despite the noticeable intersubject variability in rCBF profile, each subject's pattern is well reproduced on the repeated scan.

i.e., the lack of subject-to-subject variability in flow in other regions made it more difficult for a correlation analysis to show highly significant within-subject correlations. Thus, comparing the significance of correlation analysis as an index of reproducibility of *individual* regions is misleading for the question of what regions replicate best within subjects.

The sample size used in this study is typical of sample sizes used in many functional imaging experiments. The variance estimates should be stable and not change appreciably with larger sample sizes, even though the accuracy of the variance estimate would improve. Although somewhat arbitrary, the choice of 12 cortical ROIs per transverse section conforms relatively well with the cortical subdivisions typically referred to in state-dependent studies. The use of a greater number of ROIs might be of use in further refining these findings but should not alter the general pattern of greater between-subject variability found in the frontal regions.

There are several plausible explanations for the greater between-subject variability in relative frontal flow. It may reflect intersubject differences in mental state at the time of the scan or even hard-wired trait differences. On the other hand, it is possible that the between-subject variability is due to differences in the precise anatomical location of the SPECT slice rather than real rCBF differences at the same brain level, since the canthomeatal line is somewhat variable across subjects. However, examination of the SPECT images of two subjects with very different patterns of frontal rCBF, as in Figures 5A and 5B, indicates a consistency in this difference across almost all transverse slices. This argues against the explanation that small variations in the SPECT image's actual position above the CM line account for intersubject differences in rCBF pattern.

Independent of whether the frontal variability is rooted in anatomical, positional or behavioral differences, this data has implications for interpreting rCBF findings in disease states and in the study of activation effects. The across-subject variability in relative frontal flow creates a large range of normal rCBF with which to evaluate disease effects, suggesting that (population) criteria for frontal deficits must be fairly extreme.
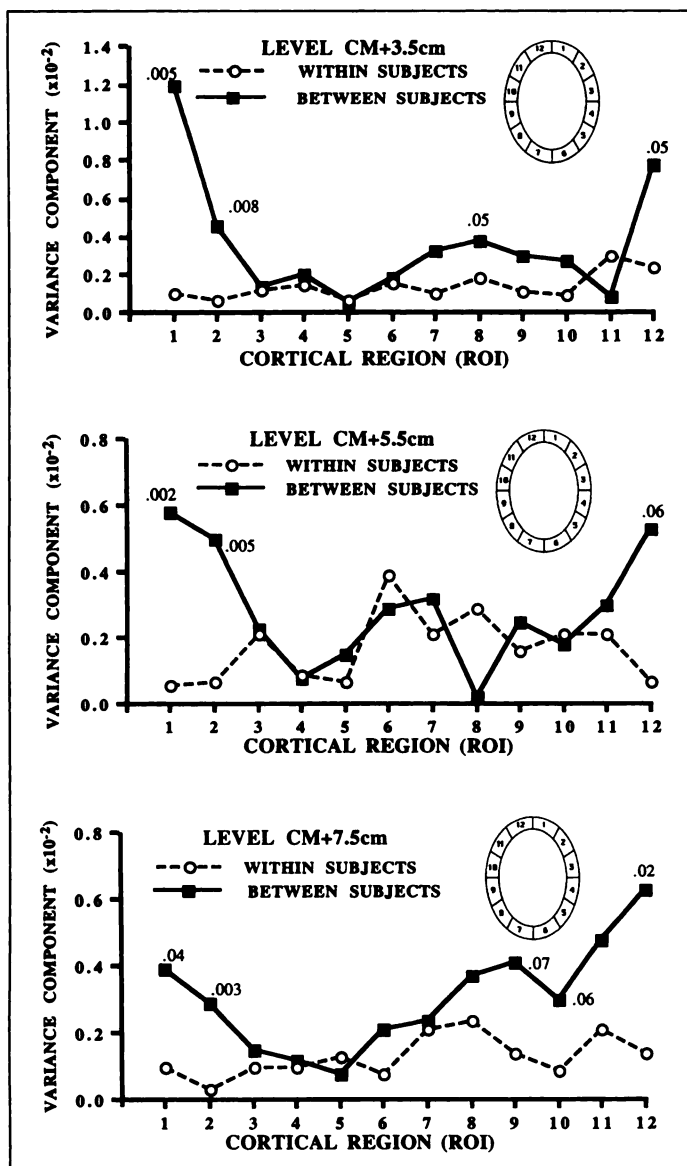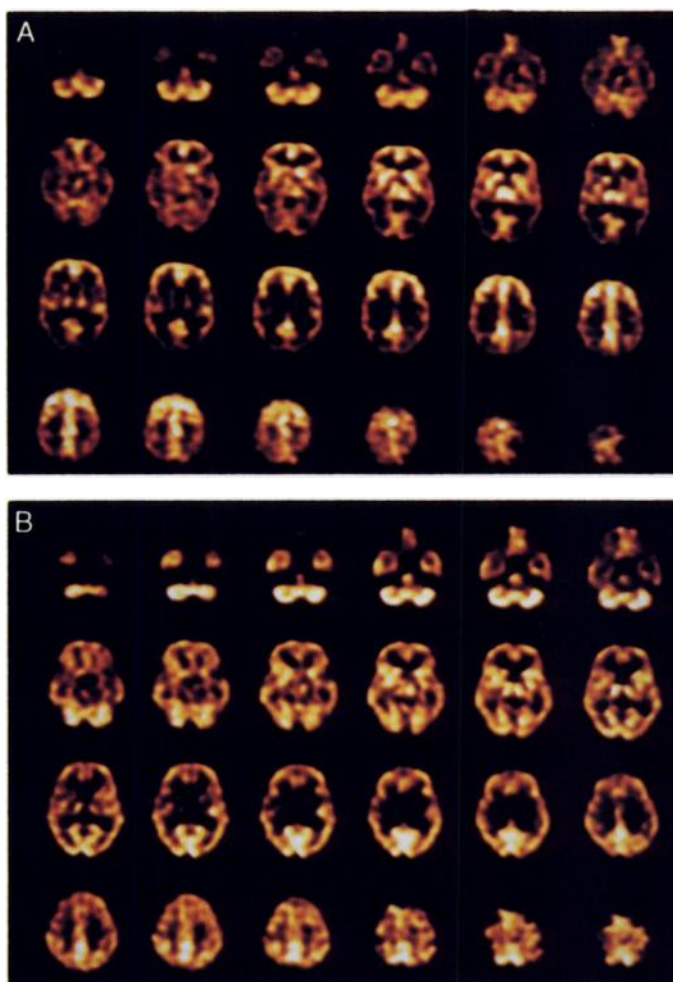
FIGURE 5. (A) Sequential ^{99m}Tc-HMPAO brain SPECT images in transverse sections for a normal 59-yr-old woman whose resting pattern of cerebral blood flow showed relatively high flows in frontal regions. (B) Transverse SPECT images of another normal woman (65-yr-old) with a different, relatively lower pattern of frontal rCBF. These figures also show the consistency in this difference between the two subjects across multiple transverse slices.

FIGURE 4. The results of variance components analysis for levels CM + 3.5, CM + 5.5 and CM + 7.5. The probability value for the difference in between- and within-subjects variance is indicated at the regions showing such differences.

Frontal flow defects have been reported in numerous disease states, a state of affairs that may be due to poor criteria as well as a lack of disease specificity to such rCBF changes (15,32). Similarly, between-subject frontal variability makes it more difficult to study state- or activation-dependent flow pattern changes and indicates the desirability of within-subject exper-

TABLE 4
Variance Components for the Subcortical Nuclei (Left and Right Caudate and Thalamus)

Structure	Between subject (raw variance $\times 10^{-3}$)	Within subject (raw variance $\times 10^{-3}$)
Lt. caudate	1.15	8.57
Rt. caudate	7.13	7.13
Lt. thalamus	1.07	8.09
Rt. thalamus	0.20	8.03

Between- and within-subjects variability was not significantly different for these structures.

imental designs in the study of frontal lobe activity changes. Thus, in addition to the well-established need of using within-subject designs to study absolute flow rates, within-subject designs are also highly preferable in assessing relative frontal lobe rCBF. On the other hand, studies of disease- or state-dependent changes in more posterior cortical regions may rely to a greater extent on group data, since the subject-to-subject variability in flow approaches that of within-subject repeated measurements.

Finally, these data bear on the issue of whether resting state scans truly help adjust for differences between subjects in the interpretation of stress and activation studies. Adjusting for resting state rCBF differences in the analysis of activation effects assumes that resting state levels reflect stable, subject specific, physiological factors that form an underlying baseline pattern within each subject upon which are superimposed the effects of any stimulation or task activity (i.e., the individual's rest pattern has a systematic affect on the pattern during activation.) Although clearly true for patients with focal defects or asymmetric flow, such as in cases of stroke, this assumption may not hold for normal subjects and many patients if inter-subject differences at rest simply reflect differences in what each subject is doing when at rest as opposed to some more permanent characteristic, e.g., anatomical, physiological or organizational differences that affect all states in some consis-

tent way. If resting state differences simply reflect idiosyncratic factors at the time of the resting scan rather than stable factors that affect all scanning conditions, then adjusting for them would hurt more than help. The results of this study, however, lend strong support to the argument that a substantial part of intersubject differences in resting rCBF are due to stable, subject-specific factors that need to be taken into account in the interpretation of stress and activation imaging protocols, thereby helping reduce the large variance typically associated with such multiple-state studies.

ACKNOWLEDGMENTS

REFERENCES

1. Kuzniecky R, Mountz JM, Wheatly G, Morawetz R. Ictal single photon emission computed tomography demonstrates localized epileptogenesis in cortical dysplasia. *Ann Neurol* 1993;34:627–631.
2. Modell J, Mountz JM. Focal cerebral blood flow change during craving for alcohol measured by SPECT. *J Neuropsyc Clin Neurosci* 1995;7:15–22.
3. Mountz JM, Tolbert LC, Lill DW, Katholi CR, Liu H-G. Functional deficits in autistic disorder: characterization by ^{99m}Tc-HMPAO and SPECT. *J Nucl Med* 1995;36:1156–1162.
4. Warach S, Gur RC, Gur RE, Skolnick BE, Obrist WD, Reivich M. Decreases in frontal and parietal lobe regional cerebral blood flow related to habituation. *J Cereb Blood Flow Metab* 1992;12:546–553.
5. Deutsch G, Papanicolaou AC, Bourbon WT, Eisenberg HM. Cerebral blood flow evidence of right frontal activation in attention demanding tasks. *Intern J Neuroscience* 1987;36:23–28.
6. Deutsch G, Bourbon TB, Papanicolaou AC, Eisenberg HM. Visuospatial tasks compared via activation of regional cerebral blood flow. *Neuropsychologia* 1988;26: 445–452.
7. Strother SC, Anderson JR, Schaper KA, Sidtis JJ, Liow J-S, Woods RP, Rottenberg DA. Principal component analysis and the scaled subprofile model compared to intersubject averaging and statistical parametric mapping: I. "Functional connectivity" of the human motor system studied with [^{15}O]water PET. *J Cereb Blood Flow Metab* 1995;15:738–753.
8. Fox PT, Mintun MA, Reiman EM, Raichle ME. Enhanced detection of focal brain responses using intersubject averaging and change-distribution analysis of subtracted PET images. *J Cereb Blood Flow Metab* 1988;8:642–653.
9. Friston KJ, Frith CD, Liddle PF, Dolan RJ, Lammertsma AA, Frackowiak RSJ. The relationship between global and local changes in PET scans. *J Cereb Blood Flow Metab* 1990;10:458–466.
10. Friston KJ, Frith CD, Liddle PF, Frackowiak RSJ. Functional connectivity: the principal component analysis of large (PET) datasets. *J Cereb Blood Flow Metab* 1993;13:5–14.
11. Strother SC, Kanno I, Rottenberg DA. Principal component analysis, variance partitioning and "functional connectivity." *J Cereb Blood Flow Metab* 1995;15:353–360.
12. Blauenstein UW, Halsey JH, Wilson EM, Wills, EL, Risberg J. Xenon-133 inhalation method, analysis of reproducibility: some of its physiological implications. *Stroke* 1977;8:92–102.
13. Prohovnik I, Hakansson K, Risberg J. Observations on the functional significance of regional cerebral blood flow in "resting" normal subjects. *Neuropsychologia* 1980;18: 203–217.
14. Deutsch G, Papanicolaou AC, Eisenberg HM, Loring DW, Levin HS. CBF gradient changes elicited by visual stimulation and visual memory tasks. *Neuropsychologia* 1986;24:283–287.
15. Deutsch G, Eisenberg HM. Frontal blood flow changes in recovery from coma. *J Cereb Blood Flow Metab* 1987;7:29–34.
16. Warach S, Gur RC, Gur RE, Skolnick BE, Obrist WD, Reivich M. The reproducibility of the ^{133}Xe inhalation technique in resting studies: task order and sex related effects in healthy young adults. *J Cereb Blood Flow Metab* 1987;7:702–708.
17. Frackowiak RSJ, Lenzi G-L, Jones T, Heather JD. Quantitative measurement of regional cerebral blood flow and oxygen metabolism in man using ^{15}O and positron emission tomography: theory, procedure and normal values. *J Comput Assist Tomogr* 1980;4:727–736.
18. Fox PT, Raichle ME. Stimulus rate dependence of regional cerebral blood flow in the human striate cortex demonstrated by positron emission tomography. *J Neurophysiol* 1984;5:1109–1120.
19. Cameron O, Agranoff B, Hichwa R, Hutchins G, Koeppe K, Kumar A. A comparison of two ambient PET scanning conditions on LCBF, using a test-retest paradigm. *J Cereb Blood Flow Metab* 1987;7(suppl 1):S590.
20. Matthew E, Andreason P, Carson RE, et al. Reproducibility of resting cerebral blood flow measurements with ^{15}O-water positron emission tomography in humans. *J Cereb Blood Flow Metab* 1993;13:728–754.
21. Holm S, Madsen PL, Sperling B, Lassen NA. Use of ^{99m}Tc-bicisate in activation studies by split-dose technique. *J Cereb Blood Flow Metab* 1994;14(suppl 1):S115–S120.
22. Anderson AR, Friberg H, Lassen NA, Kristensen K, Neirinckx RD. Serial studies of cerebral blood flow using ^{99m}Tc-HMPAO: a comparison with ^{133}Xe. *Nucl Med Commun* 1987;8:547–557.
23. Wilson MW, Mountz JM. A reference system for neuroanatomical localization on functional reconstructed cerebral images. *J Comp Asst Tomogr* 1989;13:174–178.
24. Mountz JM, Wilson MW, Wolff CG, Deutsch G, Harris JM. Validation of a reference method for correlation of anatomic and functional brain images. *Computerized Medical Imaging and Graphics* 1994;18:163–174.
25. Mountz JM, Zhang B, Liu H-G, Inampudi C. A reference method for correlation of anatomic and functional brain images: validation and clinical applications. *Sem Nucl Med* 1994;24:256–271.
26. Liu HG, Harris JM, Inampudi CS, Mountz JM. Optimal reconstruction filter parameters for multiheaded brain SPECT: dependence on count activity. *J Nucl Med Technol* 1995;23:251–257.
27. Mountz JM. Quantification of the SPECT brain scan. In: Freemen LM, ed. *Nuclear Medicine Annual.* New York: Raven Press; 1991:67–98.
28. Mountz JM, Bradley LA, Modell JG, et al. Fibromyalgia in women. *Arthritis Rheum* 1995;38:926–938.
29. Mountz JM, Deutsch G, Khan SH. Regional cerebral blood flow changes in stroke imaged by ^{99m}Tc-HMPAO SPECT with corresponding anatomic image comparison. *Clin Nucl Med* 1993;18:1067–1082.
30. Mountz JM, Deutsch G, Kuzniecky R, Rosenfeld SS. Brain SPECT: 1994 update. In: Freemen LM, ed. *Nuclear Medicine Annual.* New York: Raven Press; 1994:1–54.
31. Rodriguez G, Warkentin S, Risberg J, Rosadini G. Sex differences in regional cerebral blood flow. *J Cereb Blood Flow Metab* 1988;8:783–789.
32. Deutsch G. The nonspecificity of frontal dysfunction in disease and altered states: cortical blood flow evidence. *Neuropsychiat Neuropsychol Behav Neurol* 1992;5:301–307.